J. Am. Ceram. Soc., 97 [4] 1065–1073 (2014)
DOI: 10.1111/jace.12861

journal

Development and Characterization of Biphasic Hydroxyapatite/β-TCP Cements

Sara Gallinetti,[‡,§,¶] Cristina Canal,[‡,§,¶] and Maria-Pau Ginebra[‡,§,¶,†]

[‡]Biomaterials, Biomechanics and Tissue Engineering Group, Department of Materials Science and Metallurgy, Technical University of Catalonia (UPC), Barcelona 08028, Spain

[§]Biomedical Research Networking Center in Bioengineering, Biomaterials and Nanomedicine (CIBER-BBN), Barcelona, Spain

[¶]Center for Research in Nanoengineering (CRnE), UPC, Barcelona 08028, Spain

Biphasic calcium phosphate bioceramics composed of hydroxyapatite (HA) and β-tricalcium phosphate (β-TCP) have relevant properties as synthetic bone grafts, such as tunable resorption, bioactivity, and intrinsic osteoinduction. However, they have some limitations associated to their condition of high-temperature ceramics. In this work self-setting Biphasic Calcium Phosphate Cements (BCPCs) with different HA/β-TCP ratios were obtained from self-setting α-TCP/β-TCP pastes. The strategy used allowed synthesizing BCPCs with modulated composition, compressive strength, and specific surface area. Due to its higher solubility, α-TCP was fully hydrolyzed to a calcium-deficient HA (CDHA), whereas β-TCP remained unreacted and completely embedded in the CDHA matrix. Increasing amounts of the non-reacting β-TCP phase resulted in a linear decrease of the compressive strength, in association to the decreasing amount of precipitated HA crystals, which are responsible for the mechanical consolidation of apatitic cements. Ca^{2+} release and degradation in acidic medium was similar in all the BCPCs within the timeframe studied, although differences might be expected in longer term studies once β-TCP, the more soluble phase was exposed to the surrounding media.

I. Introduction

The increase in life expectancy in developed countries has led to higher incidence of bone fractures and other musculoskeletal disorders related to degenerative diseases such as osteoarthritis or osteoporosis. Although autografts, allografts, and xenografts have been used in clinical practice with success, all of them have drawbacks[1] and the design of synthetic biomaterials with osteogenic properties remains an open challenge.[2] In this context, calcium phosphates are promising materials, due to their similarity to the mineral phase of bone.[3,4]

Biphasic Calcium Phosphates (BCPs) were introduced in the late 1980s[5] in an effort to design synthetic bone grafts with tunable resorption rate. They are composed of Hydroxyapatite (HA), the most stable calcium orthophosphate (solubility at 25°C, −log (Ks) = 116.8), and β-Tricalcium phosphate (β-TCP), a more soluble compound (solubility at 25°C, −log (Ks) = 28.9),[6] with varying HA/β-TCP ratios. The resorption and bioactivity of BCPs can be controlled by changing the HA/β-TCP ratio and the crystallinity of the ceramic.[7]

In recent years it has been shown that, in addition to being osteoconductive (promoting bone ingrowth in direct contact with their surface), BCPs are also osteoinductive, i.e., they are able to foster differentiation of stem cells to the osteogenic lineage, leading to bone induction even in a non-osseous environment. This capacity, that initially was associated to the action of some growth factors, such as bone morphogenetic proteins, can also be triggered by some materials with specific chemical and structural characteristics.[8–10] This is the case of BCPs, where a proper combination of chemical composition, macroporosity, and microporosity has been shown to promote osteogenesis *in vivo*,[11,12] even without the addition of exogenous growth factors. In addition to specific microstructural features, the higher release of Ca^{2+} ions by BCPs when compared with pure HA is proposed to be one of the parameters that explain the higher osteoinductive potential of this group of materials.[12,13]

Biphasic Calcium Phosphates are normally obtained by high-temperature sintering of calcium-deficient apatites or other calcium phosphate precursors,[7] with the limitations associated to this type of materials, e.g., they can be obtained only as preformed ceramics or granules. The objective of this work is to obtain self-setting BCPs, which would add to the benefits of osteoinductive BCP ceramics, the advantages associated to calcium phosphate cements like mouldability or injectability. It is known that α-tricalcium phosphate [α-TCP, solubility at 25°C, −log (Ks) = 25.5] hydrolyses to a calcium-deficient HA (CDHA) upon setting.[14] Our hypothesis was that a biphasic HA/β-TCP material could be obtained from a mixture of α-TCP and the less soluble polymorph β-TCP, upon reaction with an aqueous solution. In the study, the properties of new biphasic calcium phosphate cements (BCPCs) with different α-TCP/β-TCP ratios were characterized, paying special attention to the setting reaction, mechanical properties, degradation, and ion release.

II. Experimental Procedure

(1) α-TCP and β-TCP Preparation and Characterization

Alpha-tricalcium phosphate (α-$Ca_3(PO_4)_2$, α-TCP) was obtained by heating calcium hydrogen phosphate ($CaHPO_4$; Sigma Aldrich C7263, St. Louis, MO) and calcium carbonate ($CaCO_3$; Sigma Aldrich C4830) at a molar ratio of 2:1, at 1400°C for 2 h, followed by quenching in air. Beta-tricalcium phosphate [β-$Ca_3(PO_4)_2$, β-TCP] was obtained by heating for 5 h at 1100°C the same reactants and slow cooling to room temperature.

Subsequently, α-TCP and β-TCP were milled in an agate ball mill (Volume of the jar = 500 mL) (Pulverisette 6, Fritsch

J. Ferreira—contributing editor

Manuscript No. 33441. Received June 28, 2013; approved January 20, 2014.
†Author to whom correspondence should be addressed.
e-mail: maria.pau.ginebra@upc.edu

GmbB Idar-Oberstein, Germany). The milling protocols were adjusted to obtain similar particle size distributions in both powders. Given the different crystal structures of the two polymorphs, together with the different initial grain size due to different thermal treatments, to obtain similar particle size a different milling protocol had to be implemented for each polymorph. Thus, α-TCP was milled at 450 rpm for 15 min, with a weight ratio powder/balls = 0.50, and β-TCP was milled at 150 rpm for 60 min, with a weight ratio powder/balls = 0.42, using 10 agate balls (d = 30 mm) in both cases.

The particle size distribution of the powder was measured by laser diffraction (LS 13 320 Beckman Coulter, Brea, CA). The powder was previously dispersed in ethanol in an ultrasonic bath to avoid the presence of agglomerates during measurement. Specific Surface Area (SSA) was determined by Nitrogen Adsorption following the Brunnauer–Emmet–Teller method (BET) in an ASAP 2020 (Micromeritics, Norgross, GA). Phase composition was assessed by X-ray powder diffraction (XRD; PANalytical, X'Pert PRO Alpha-1) by scanning in Bragg-Brentano geometry using CuK_α radiation (λ = 1.5406 A). The experimental conditions used were 1.5 h of scan time with 2θ scan step of 0.020° and scan range between 4° and 100°, with measuring time of 50 s per step. X-ray generator parameters: voltage 45 kV and intensity 40 mA. To analyze BCPCs the samples were crushed to powder with a mortar. The diffraction patterns were compared with the Joint Committee on Powder Diffraction Standards for α-TCP (JCPDS No. 9–348), β-TCP (JCPDS No. 9–169) and HA (JCPDS No. 9–432).[15] Rietveld refinements were carried out in triplicate to quantify the phases present. The Inorganic Crystal Structure Database was used, including structural models for α-TCP (ICSD no. 923), b-TCP (ICSD no. 6191), and HA (ICSD no. 151414).[16]

The presence of an amorphous phase was assessed by the external standard method, adding a known amount of a zinc oxide standard (Panreac 141786-1210, Barcelona, Spain) to the different studied powders. Rietveld refinements were carried out using the FullProf Suite software package to quantify the phases present using the Inorganic Crystal Structure Database (ICSD) including structural models for α-TCP (ICSD no. 923), β-TCP (ICSD no.6191), HA (ICSD no. 151414), and ZnO (ICSD no. 26170).

(2) Biphasic Cement Preparation

Biphasic cements (BCPCs) were prepared by mixing the powder, consisting of combinations of α-TCP and β-TCP in various proportions, with an aqueous solution of 2 wt% Na_2HPO_4 (Panreac) at a L/P ratio of 0.35 mL/g. Subsequently, the cement paste was put in Teflon moulds and immersed in Ringer's solution at 37°C for 7 d to allow the complete reaction of the cement. Hereafter, the biphasic CPCs will be named according to the amount of β-TCP (0, 20, 40, 60, 80, and 100 wt% β-TCP).

(3) Cement Characterization

The initial and final setting times of the cement pastes were determined with Gillmore needles according to the C266-ASTM standard.[17] The cohesion time was determined by visual inspection after immersion of the samples in deionized water at 37°C.[18]

The compressive strength was evaluated in cylindrical specimens (12 mm height × 6 mm diameter) at a cross-head speed of 1 mm/min using a Servohydraulic Testing Machine MTS BIONIX 358 (Eden Prairie, MN). Six replicates were prepared for each cement formulation. The surface microstructure of the BCPCs coated with Au was investigated by Field Emission Scanning Electron Microscopy (FE-SEM; Hitachi H-4100FE, Tokyo, Japan).

To ascertain the bulk microstructure of 0% and 80% β-TCP cements, Focus Ion Beam tomography (FIB; Zeiss Neon40, Oberkochen, Germany) was performed. A 30 μm × 30 μm × 25 μm parallelepiped was cut, coated with Au–Pd and cut in slices and FE-SEM pictures were taken to reconstruct the 3D material structure.

The SSA of the BCPCs was measured by Nitrogen adsorption according to the Brunauer–Emmet–Teller (BET) method, and the cement phase composition was evaluated by X-ray diffraction analysis (XRD; Philips MRD, Almelo, The Netherlands) and studied by Rietveld refinement as described in section II (1).

The porosity and pore entrance size distribution was measured by mercury intrusion porosimetry (MIP; Autopore IV 9500, Micromeritics).

(4) Ion Release and Accelerated in vitro Degradation Test

Set BCPC discs (2 mm height × 15 mm diameter) were prepared and introduced in 1.5 mL of MilliQ water. At different time points of 2, 6, 10, 24, 48, and 72 h the samples were removed and the Calcium concentration in the media was analyzed with an Ion-selective electrode (ILyte Na/K/Ca/pH, Instrumentation Laboratory, Bedford, MA). Three replicates of each formulation were prepared and measured at each time point.

In vitro degradation of BCPCs was evaluated under accelerated conditions in acidic solution during 8 h.[19,20] Set discs (2 mm height × 15 mm diameter, which accounts for an apparent surface of 447 mm^2) were prepared and dried in an oven at 120°C until constant weight. A control consisting of 100% β-TCP compacted discs was also evaluated, with the aim of assessing if the fact of using as-milled powders instead of hydrated ones had some effect on the dissolution rate of pure β-TCP. The compacted discs (2.7 mm height × 9 mm diameter) were prepared by compressing β-TCP powders (0.5 g) at 10 kN, for 10 s. To maintain a total apparent surface similar to the BCPC samples, two β-TCP compacted discs were used for each experiment (accounting for an apparent surface of 407 mm^2).

Each sample was introduced in 50 mL of a pH 2 aqueous solution (0.01M HCl and 0.14M NaCl) at 37°C. The medium was refreshed every hour and the specimens were weighted after carefully removing remaining droplets on the surface using a wet paper. The assay was performed in triplicate for 8 h. After the assay, samples were dried in the oven at 120°C until constant weight to calculate the weight loss. Given the low pH of the solutions, the ion-selective electrode could not be used, and the concentration of calcium at each time point was obtained by reaction with ortho-cresolphthalein complexone (OCPC, Sigma-Aldrich®) to obtain a colored solution[20] which was measured by absorbance in a UV–vis spectrometer (Infinite M200 Pro Microplate Reader; TECAN, Männdorf, Switzerland). The values were normalized to the initial sample weight.

(5) Statistics

Statistical differences were determined using one-way ANOVA with Tukey's post-hoc test (95%) using Minitab software (Minitab Inc, State College, PA). Statistical significance was noted when $P < 0.05$.

III. Results

(1) Powder Characterization

The XRD patterns of the α-TCP and β-TCP powders are shown in Fig. 1, together with their particle size distribution, as determined by laser diffraction. The two powders consisted mostly of α-TCP (94.9%) and β-TCP (97.5%). The presence of amorphous phase was estimated to be below the limit of detection (1%) in both cases. The granulometric parameters of the powders are summarized in Table I along with the SSA values.

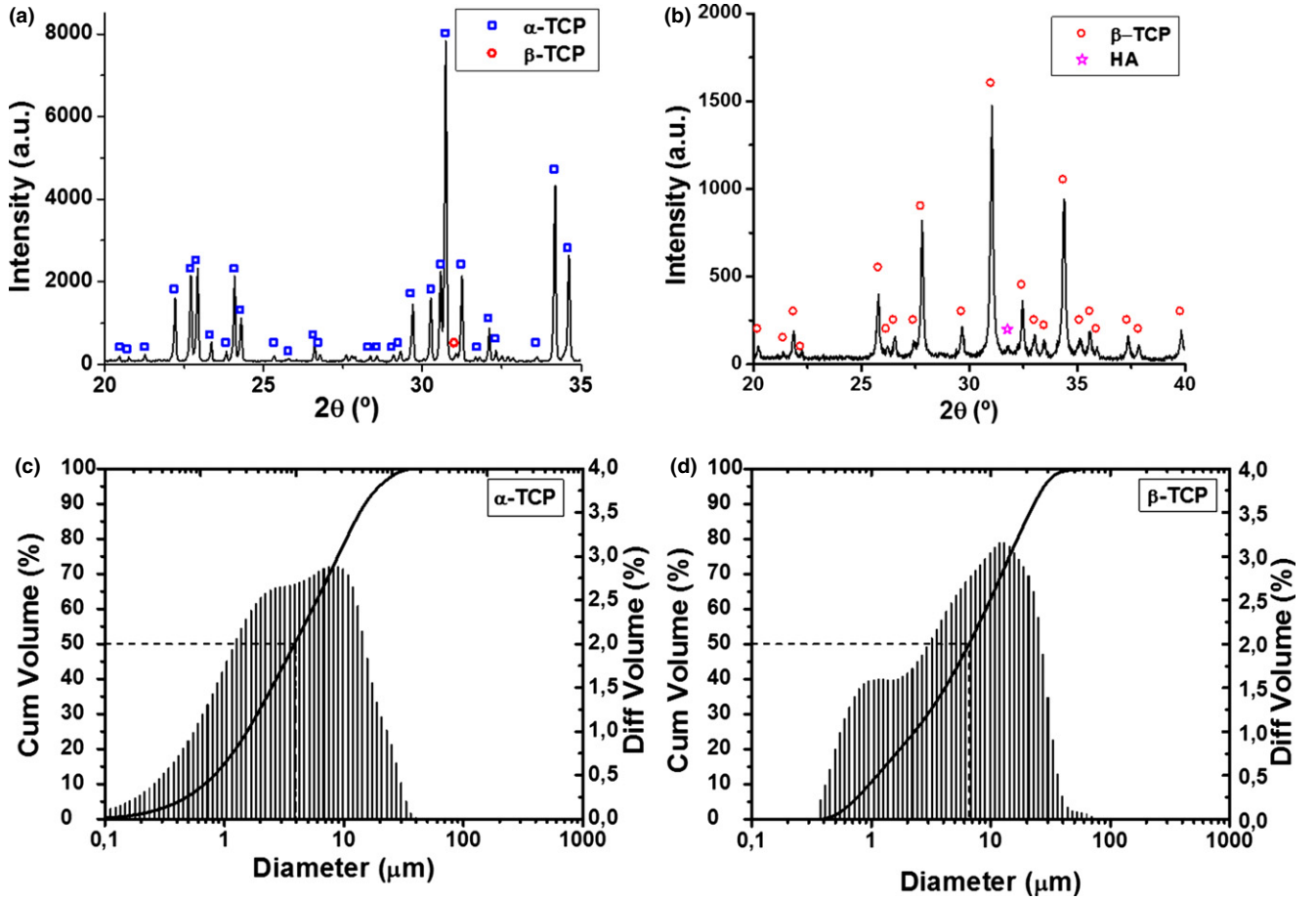

Fig. 1. X-Ray diffraction patterns of α-TCP (a) and β-TCP (b); particle size distribution of α-TCP (c) and β-TCP (d) powders. The curve indicates the cumulative volume with focus on 50% (median) and the bars correspond to the differential volume of particles.

(2) Cement Characterization

All cement formulations gave a homogeneous paste with good workability. The results obtained for the cohesion time, initial setting time and final setting time are given in Fig. 2. The cohesion time was defined as the minimum time after which the cement did not suffer disintegration when immersed in deionized water at 37°C. All cements presented cohesion in water after a few minutes, and as shown in Fig. 2, cohesion time increased by adding β-TCP, irrespective of the amount. The addition of a second phase (β-TCP) did not alter much the initial setting time but did substantially increase the final setting time. The 100% β-TCP cement showed faster cohesion than the BCPCs but the final setting time was significantly higher.

The XRD patterns of the starting BCPC powders and of the set cements after 7 d in Ringer's solution at 37°C are shown in Figs. 3 (a) and (b) respectively. The phase composition of the powder mixtures and of the BCPCs after setting as determined by Rietveld refinement is summarized in Table II. It could be observed that α-TCP was completely hydrolyzed to an apatitic phase, more specifically a CDHA,[14] whereas the amount of β-TCP remained nearly unchanged.

The compressive strength of the different BCPCs is shown in Fig. 4 (a). A linear decrease could be observed in the compressive strength of the BCPC with the increase in β-TCP amount. The total porosity slightly increased with the addition of β-TCP [Fig. 4 (c)]. The pore size distribution of the BCPCs [Fig. 4 (d)] was broad (between 6 nm—lower limit of the technique—and 3 mm for the 100% β-TCP composition). The 0% β-TCP showed a broad peak centered around

Table I. Particle Size Distribution Parameters in Volume and Specific Surface Area of α-TCP and β-TCP Reactant Powders

Material	D10 (μm)	Median size, D50 (μm)	D90 (μm)	Specific surface area SSA(m^2/g)
α-TCP	0.684	3.855	15.05	0.975 ± 0.006
β-TCP	0.963	6.561	23.04	0.739 ± 0.003

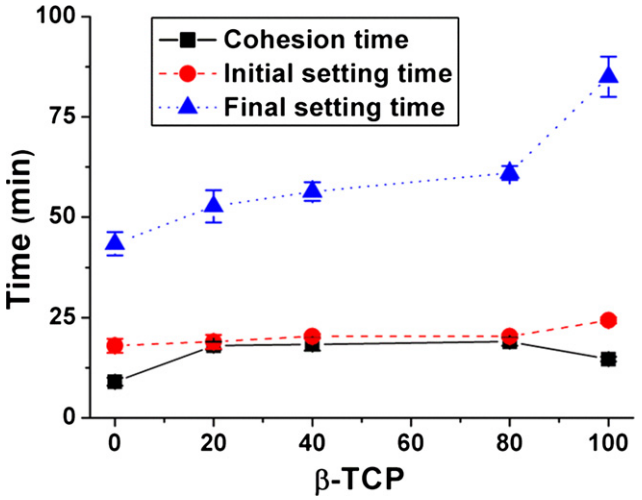

Fig. 2. Cohesion time, initial setting time, and final setting time of BCPCs composed of α-TCP and β-TCP at different ratios at a L/P = 0.35 mL/g.

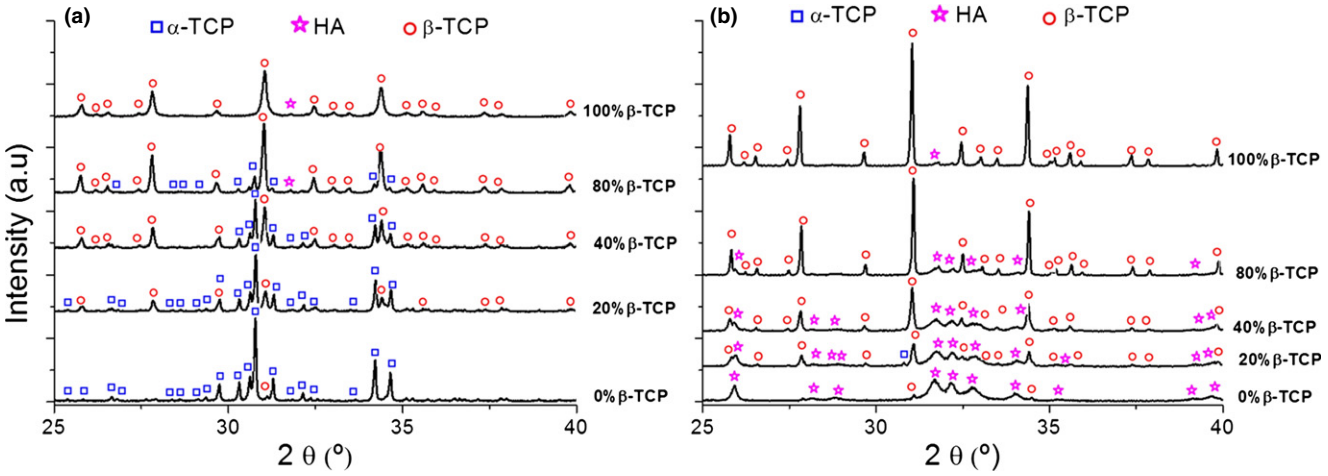

Fig. 3. X-ray diffraction patterns of the starting powders (a) and the set cements (b) for the different BCPCs, with increasing contents of β-TCP. The set cements were obtained after 7 d reaction in Ringer's solution at 37°C.

Table II. Phase Composition of the Reactants and Set Cements. The Measured Composition was Determined by Rietveld Refinement of the XRD patterns

			Initial powders			Set cements		
	Nominal composition		Measured composition (XRD/Rietveld refinement)*			Measured composition (XRD/Rietveld refinement)*		
Material	% α-TCP	% β-TCP	% α-TCP	% β-TCP	% HA	% α-TCP	% β-TCP	% CDHA
0% β	100	0	94.9	2.9	2.2	0	3.7	96.3
20% β	80	20	76.7	22.8	0.5	0	21.4	78.6
40% β	60	40	54.8	44.6	0.6	1.5	37.4	61.1
80% β	20	80	17.4	82.1	0.5	0	77.8	22.2
100% β	0	100	2.4	97.5	0.1	0	99.5	0.5

*Error ± 1%.

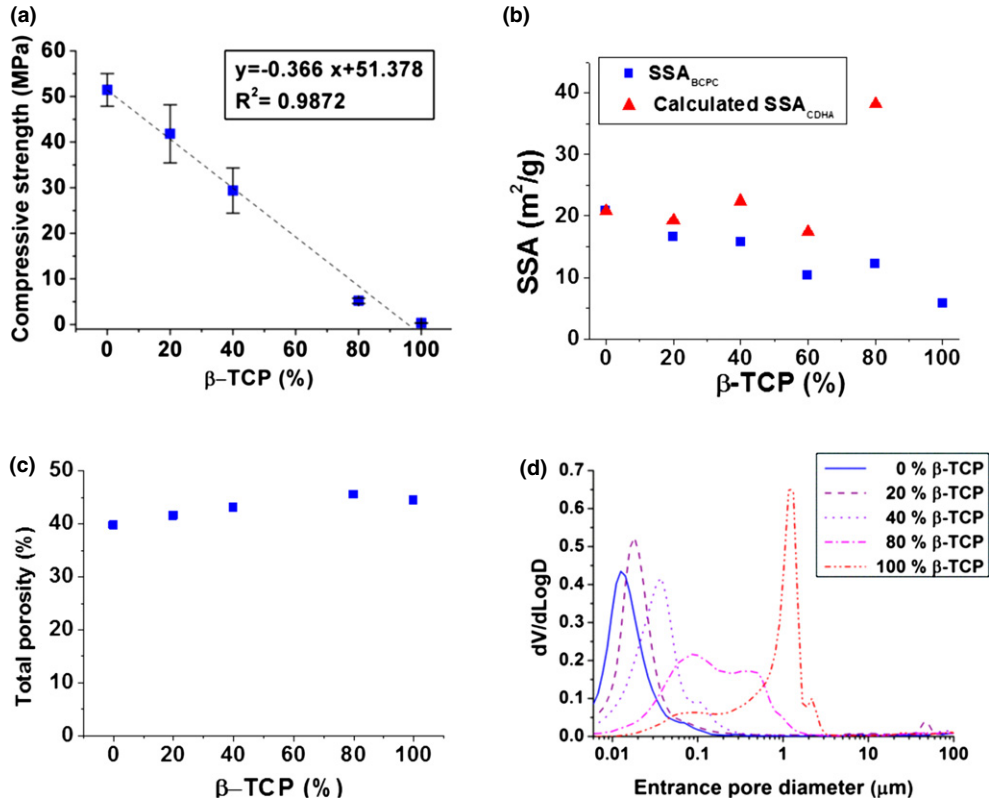

Fig. 4. Compressive strength (a) Specific Surface Area (SSA) of the BCPCs, and calculated SSA of the CDHA, according to the rule of mixtures (b), Total porosity (c), and Pore Entrance Size Distribution (d) of BCPCs with different β-TCP%.

0.01 μm, confirming previous results,[21] with a shoulder around 0.06 μm. Incorporation and progressive percentage increase of β-TCP led to a displacement of the main peak to higher values (0.02 and 0.04 μm for 20% and 40% β-TCP respectively) with an intensification of the shoulder around 0.1 μm. 80% β-TCP showed a bimodal pore size distribution with maxima at 0.1 and 0.6 μm. The first peak was still present in the 100% β-TCP although with a lower population of pores, together with a sharper peak around 2 μm.

The surface morphology of the various BCPCs observed by FE-SEM is shown in Fig. 5. The β-TCP particles were not exposed in any of the BCPCs, even those containing large amount (80%) of β-TCP, as they were completely covered with CDHA precipitated crystals. However, a change in morphology of the crystals was observed. On the surface of BCPCs containing low amounts of β-TCP (up to 40%), predominantly plate-like crystals were found [Figs. 5 (a–c)], some acicular crystals were found in the 60% β-TCP [Fig. 5(d)], and most extensively in the 80% β-TCP [Fig. 5(e)], where much smaller needle-like crystals were formed. In the 100% β-TCP sample [Fig. 5(f)], the shape of the initial β-TCP particles was visible, although partially covered with small crystals. Interestingly, in spite of these microstructural changes, the addition of β-TCP resulted in a global decrease of the SSA of the set BCPCs [Fig. 4 (b)], as it resulted from the contribution of both phases, CDHA and β-TCP.

The cross-sections obtained by FIB tomography provided relevant information (Fig. 6). In the 80% β-TCP sample [Figs. 6(a) and (b)], CDHA crystals were observed to grow on the surface of the β-TCP particles, which were fully embedded in the cement matrix. In the 0% β-TCP no particles were observed [Fig. 6(c)]. Instead, dense shells with loosely packed cores that reproduced the shape of the original α-TCP particles were found, as highlighted in Fig. 6(d). FIB videos are included as Additional Information 1 and 2.

(3) Ion Release and Accelerated in vitro Degradation

The release of calcium in deionized water by the different set BCPC formulations is represented in Fig. 7. Despite the highest solubility of β-TCP when compared with CDHA, Ca^{2+} release decreased when the amount of β-TCP in BCPCs increased.

Furthermore, accelerated acidic degradation was performed at pH = 2. Fig. 8 (a) shows the weight loss of the different BCPCs. Cements with no or low amount of β-TCP showed similar weight losses, whereas the 80% β-TCP had the lowest loss. The greatest weight loss was recorded for the cement containing 100% β-TCP and for the 100% β-TCP compacted discs, despite the fact that the apparent surface of the compacted discs was slightly smaller. The related calcium release in acidic media [Fig. 8 (b)] showed that all formulations released calcium, the concentration increasing linearly with time, and no significant differences were found among the various cements. Significantly higher amounts of Ca^{2+} release were registered only for the 100% β-TCP compacted discs.

IV. Discussion

In this work biphasic CDHA/β-TCP cements were obtained by mixing two Tricalcium Phosphate (TCP) polymorphs with different solubilities. In particular, α-TCP and β-TCP powders with particle size in the same range (Table I) were mixed in different proportions and allowed to set. In spite of the small differences in solubility, when the two polymorphs were mixed with an aqueous solution only α-TCP was completely hydrolyzed to CDHA, whereas β-TCP remained unreacted (Fig. 3, Table II). The setting of these biphasic cements based on α-TCP and β-TCP follows, therefore, the following reaction (1).

$$3\alpha - Ca_3(PO_4)_2 + 3\beta - Ca_3(PO_4)_2 + H_2O \rightarrow Ca_9HPO_4(PO_4)_5OH + 3\beta - Ca_3(PO_4)_2 \quad (1)$$

β-TCP particles acted as nucleation points, and they became embedded in the CDHA matrix as the reaction progressed, as represented in Fig. 9. This mechanism would also explain the presence of smaller needle-like crystals in the composition containing 80% β-TCP [Fig. 5(d)] because the higher amount of β-TCP provided a greater surface for heterogenic nucleation. After complete reaction, the β-TCP phase remained hidden in the structure, as evidenced by the FIB tomography for the 80% β-TCP sample [Figs. 6 (a) and (b) and Supplementary Information]. In the 0% β-TCP the

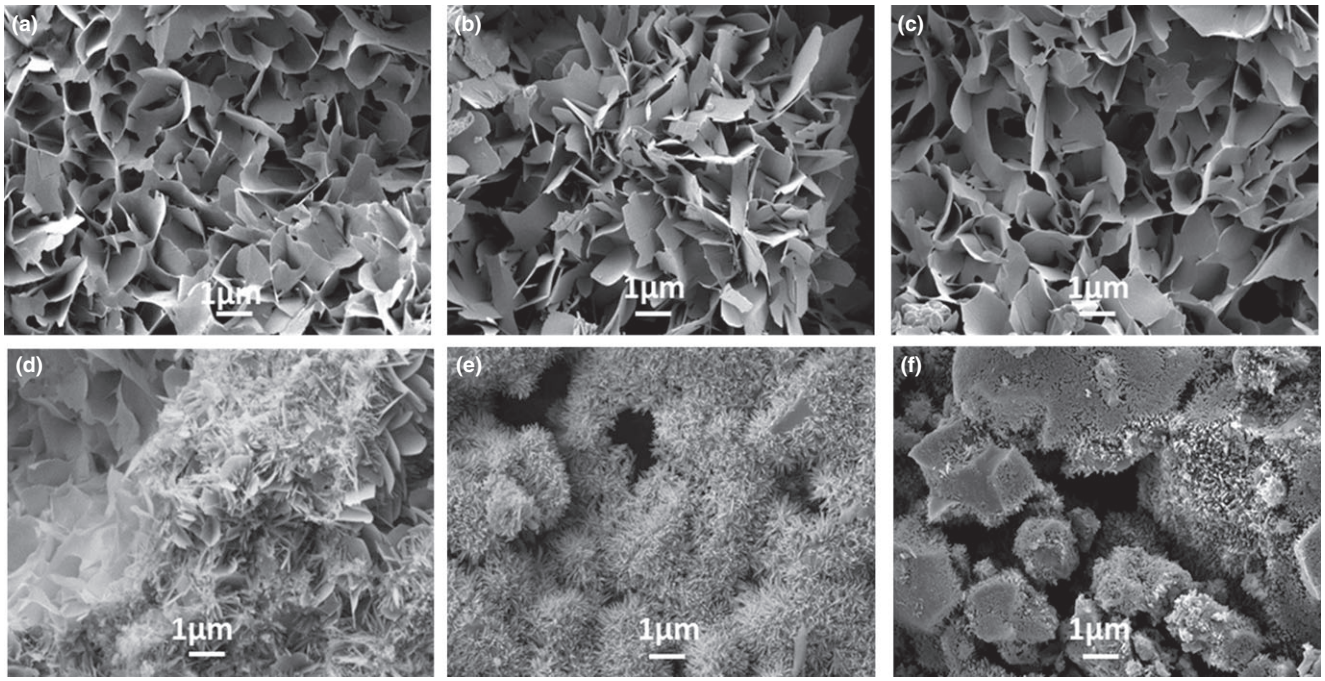

Fig. 5. Surface microstructure of BCPCs set for 7 d in Ringer's solution: (a) 0% β-TCP, b) 20% β-TCP, c) 40% β-TCP, d) 60% β-TCP, e) 80% β-TCP, f) 100% β-TCP.

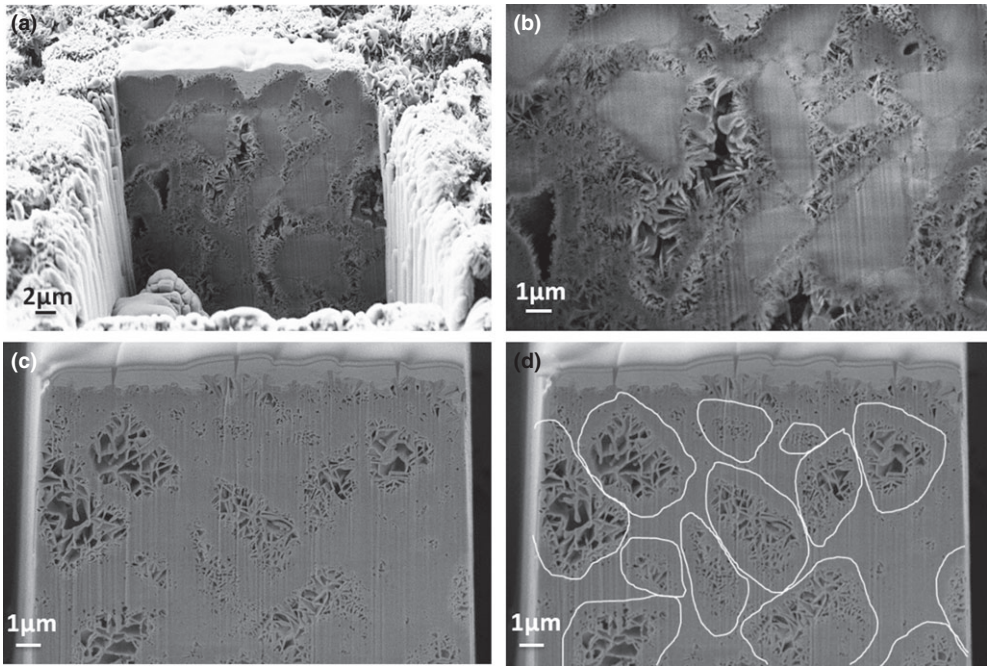

Fig. 6. (a) General view of FIB tomography of 80% β-TCP cement; (b) detail of the same specimen showing the β-TCP particles embedded in the CDHA crystals. (c) FIB tomography of the 0% β-TCP cement; (d) the same image highlighting the Hadley grains formed after hydrolysis of the initial α-TCP particles, with a dense shell and a core with bigger and loose crystals, where the size and morphology of the original particles can be estimated. All specimens were previously set for 7 d in Ringer's solution.

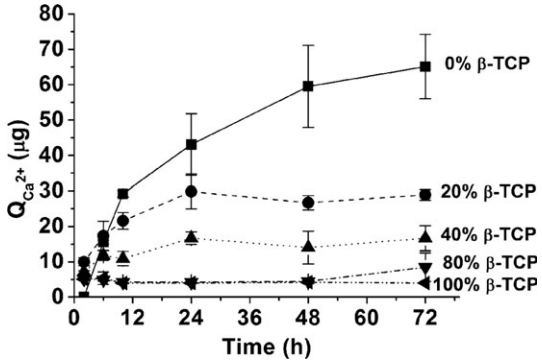

Fig. 7. Calcium release of different set BCPCs immersed in deionized water over 72 h. The BCPCs were previously set for 7 d in Ringer's solution at 37°C.

FIB tomography evidenced the presence of shell-like structures formed during the hydration of the α-TCP particles [Figs. 6 (c) and (d)],[21,22] which were analogous to the Hadley grains produced during hydration of Portland cement.[23,24]

The presence of small precipitated crystals observed by SEM in the 100%β-TCP sample [Fig. 5(e)], consistent with the five-fold increase in SSA [Table I and Fig. 4(b)] could be attributed to the hydrolysis of the small percentage of α-TCP in the initial powder (Table II), and probably also to the dissolution and reprecipitation of the more external layer of the β-TCP particles that were subjected to an amorphization due to the milling, understood not in the sense of a new phase, but to the introduction of defects and dislocations in the crystal network, which increased their reactivity, as previously reported.[25–29] In fact, although the formation of CDHA was not detected by XRD, presumably due to its small amount and low crystallinity, a narrowing

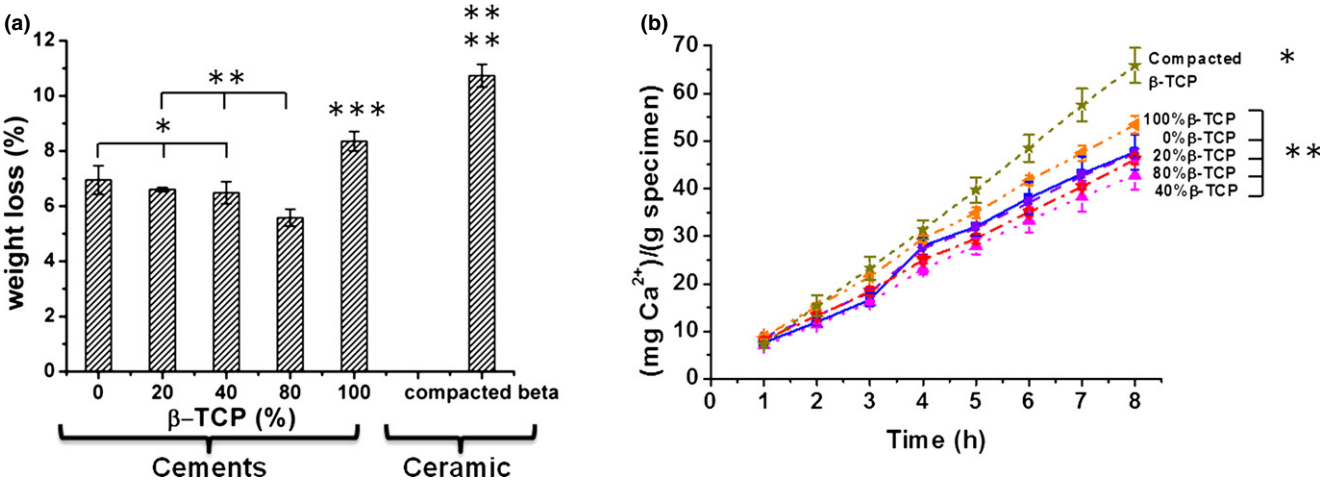

Fig. 8. Acid degradation assay (8 h, pH = 2): (a) Weight loss (b) Ca^{2+} release normalized to the sample weight. BCPCs with different amounts of β-TCP, ranging from 0% to 100%, and compacted β-TCP powders were analysed. The BCPCs were previously set for 7 d in Ringer's solution at 37°C. Differences were considered statistically significant at $P < 0.05$. Series with statistically significant differences are marked with different number of asterisks.

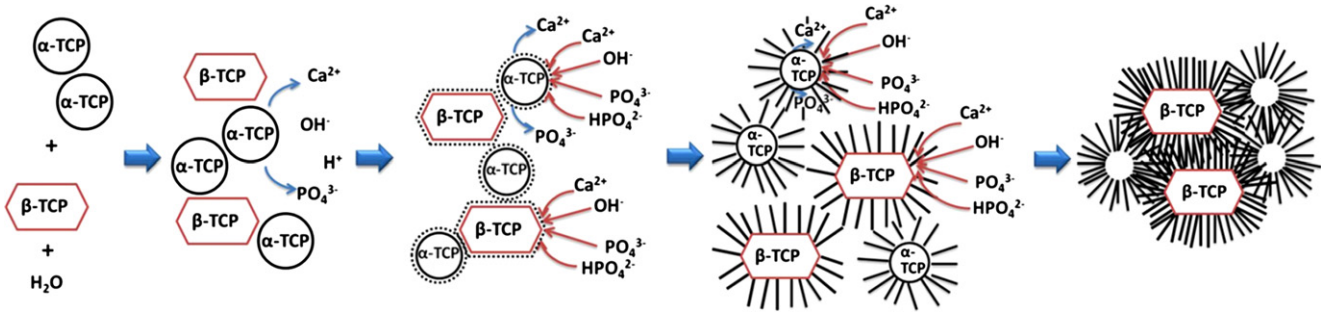

Fig. 9. Proposed dissolution-precipitation mechanisms involved in BCPCs cements prepared with α-TCP and β-TCP. In contact with water, only α-TCP starts dissolving, followed by CDHA precipitation around both α-TCP and β -TCP and subsequent crystal growth.

and higher intensity of the β-TCP peaks was observed after 7 d immersion in Ringer's solution (Fig. 3), which could be attributed to the dissolution of the partially amorphized surface of the β-TCP particles, as reported in previous works.[28]

The addition of a non-reacting phase (β-TCP) modified significantly various cement parameters, albeit to different extents. In particular, initial setting times and cohesion were not greatly modified. However, the final setting times clearly increased with the addition of β-TCP, which was consistent with the limited reactivity of this phase. The fact that the 100% β-TCP cement showed also cohesion and an apparent setting could be explained by the powder activation produced by ball milling, as discussed in the previous paragraph,[24–29] together with the presence of small amounts of α-TCP, which led to the partial dissolution of the particles, although limited to the most external surface.

The hardening mechanism of α-TCP-based cements was due to the entanglement of the precipitated CDHA crystals. Previous studies by Ginebra *et al.*[14] demonstrated a direct correlation between compressive strength and % of precipitated CDHA. Thus, the progressive reduction of compressive strength with higher β-TCP percentages in the BCPC [Fig. 4(a)] could be related to the decreasing amount of CDHA with increasing β-TCP amounts, and therefore it could be concluded that the β-TCP particles embedded in the cements, rather than reinforcing the material, had a weakening effect.

These results were obtained using small β-TCP particles, with sizes and grading similar to those of the α-TCP phase, with the idea of favoring β-TCP dissolution. The properties of the non-reacting phase, like particle size, shape, and surface texture were expected to have an effect on the properties of both freshly mixed and hardened cements, although this was beyond the scope of this study. This in fact was extensively studied in the case of concrete, where a non-reactive phase (i.e., the aggregate), was embedded in the reacting matrix (i.e., the cement). Aggregate properties were known to affect workability and rheological properties of the paste and also the mechanical performance of the hardened paste.[30] Thus, the use of particles with different sizes was shown to be more effective than monodisperse particles because of a higher packing efficiency. Bigger aggregate sizes resulted in higher fracture energy,[31] and rough-textured, angular, and elongated particles required more water to produce workable pastes than smooth, rounded particles, this affecting also the final mechanical properties of the material.[30,31]

The addition of β-TCP also led to a decrease of SSA of the BCPCs [Fig. 4(b)], as a direct consequence of the lower SSA of the β-TCP particles when compared with the precipitated CDHA crystals. This is compatible with the lower size of the CDHA crystals observed in Fig. 5 (f). In fact, the total SSA of the material results from the contribution of two different phases, CDHA and β-TCP, following the rule of mixtures:

$$SSA_{BCPC} = X_{CDHA}.SSA_{CDHA} + X_{\beta-TCP}.SSA_{\beta-TCP} \quad (2)$$

where X is weight fraction of each of the components. If we assume that SSA of β-TCP is constant during the whole process (it suffers only a very limited surface dissolution), then we can estimate a calculated SSA of the CDHA:

$$SSA_{CDHA} = (SSA_{BCPC} - X_{\beta-TCP} \cdot SSA_{\beta-TCP})/1 - X_{\beta-TCP} \quad (3)$$

As shown in Fig. 4(b), there was a drastic increase of the estimated SSA of CDHA for the sample with 80% β-TCP, which was in accordance with the SEM images that showed an evolution of the microstructure from plate-like to needle-like crystals (Fig. 5).

The porosity of BCPCs increased with growing amounts of β-TCP, as well as the entrance pore size [Fig. 4 (c) and (d)]. Interestingly, a significant change in the MIP curves was found in the group with 80% β-TCP, which can be explained by the fact that in this material the reacting phase, which accounted for only 20% of the total, was unable to fill the large voids between the β-TCP particles, as shown in Figs. 6 (a) and (b).

The dissolution behavior of the biphasic materials is relevant not only when considering the resorption behavior of the material *in vivo*, but also the ion exchange patterns, which have been shown to affect several signaling pathways relevant for osteogenesis. In fact, it has been shown recently that Ca^{2+} plays an essential role in bone remodeling processes. High Ca^{2+} concentrations are shown to stimulate pre-osteoblast chemotaxis to the site of bone resorption, and their maturation into cells that produce new bone.[13,32] This has been hypothesized to be behind the osteoinductive properties of some BCP ceramics. Therefore, the effect of varying amounts of β-TCP on the release profile of calcium from the BCPCs was studied. After the setting reaction, biphasic CDHA/β-TCP materials were obtained. CDHA was more soluble than stoichiometric HA (solubility at 25°C, −log (Ks) = ~85.1 when compared with 116.8 for HA) and less than β-TCP (solubility at 25°C, −log(Ks) = 28.9).[6]

Surprisingly, Ca^{2+} release in water was higher in the set 0% β-TCP cement, consisting in pure CDHA, and decreased with increasing amounts of β-TCP in the material, i.e., when the CDHA/β-TCP ratio decreased (Fig. 7). This result could seem to be in contradiction with the fact that CDHA was less soluble than β-TCP, and also with the behavior found in BCP ceramics composed of HA/β-TCP, where the higher the ratio, the lower was the extent of dissolution.[7] Moreover, the total porosity increased slightly, and the pore entrance size also tended to increase with higher contents of β-TCP [Figs. 4 (c) and (d)]. The behavior observed can be explained by three factors: (i) β-TCP remained hidden within the CDHA matrix, which impaired the contact with surrounding media [Fig. 6 (b)]; (ii) the precipitated CDHA had a very

low crystallinity, which was known to increase solubility, thus reducing the difference with the solubility of β-TCP; and (iii) the decreasing SSA of the BCPC with increasing β-TCP content, due to the lower SSA of β-TCP when compared with CDHA.

In general the solubility of calcium phosphates was strongly affected by pH, it was more soluble in acidic environment.[32] This mechanism was exploited by osteoclasts, which triggered bone resorption by dissolving the hydroxyapatite contained in bone through the acidification of the extracellular fluids. In fact, Silver *et al*. found that a pH decrease of about 1 unit/min took place in the sealed regions under the osteoclasts known as resorption lacunae.[33] Following the model proposed by Hankermeyer *et al*., in here, the accelerated degradation of BCPCs was studied at pH = 2.[19] The Ca^{2+} release in acidic medium was similar for all BCPCs, in spite of the different compositions (Fig. 8). Again, even in acidic conditions the microstructure and the textural properties were more determining factors than the solubility of the different phases present in the material, as no differences were observed between the different BCPCs, and a higher weight loss was found only for the 100% β-TCP cement. Interestingly, even though the apparent surface was slightly smaller, significantly higher values of weight loss and Ca^{2+} release were recorded for the as-milled compacted β-TCP discs than for the 100% β-TCP cement. This could be associated to two different phenomena: (i) the increase in powder reactivity in the as-milled powder, due to some degree of amorphization of the surface of the particles produced during milling, understood not as the formation of a distinct amorphous phase, but to the introduction of defects in the crystal structure, which made the particles more reactive, as observed in previous studies[25–29]; (ii) the loss of reactivity of the β-TCP powder which was mixed with water induced dissolution of the amorphous fraction of the mechanically activated surface of the particles and subsequent reprecipitation, leading to the formation of a CDHA layer on the surface of the particles of the 100% β-TCP cement [Fig. 5(f)]. This layer, although very thin, hindered further dissolution of the particles.[34]

In a previous work Lopez-Heredia *et al*.[35] obtained calcium phosphate cements, containing α and β-TCP phases in dual form in the same granule. To this end, various thermal treatments were applied to α-TCP to obtain different degrees of conversion to β-TCP, so particles containing both polymorphs in different ratios were used as powder phase for the preparation of cements. Although their cement formulations were far more complex than the ones analyzed in this study, they contained other phases in addition to TCPs, such as anhydrous dicalcium phosphate and precipitated hydroxyapatite, similar trends were found in terms of the reduction of SSA and compressive strength with increasing content of β-TCP. No differences were found after 8 weeks in the *in vivo* behavior when multiphasic cements containing either dual TCP phases or only α-TCP were implanted in tibial intramedullary cavities in guinea pigs. Although only one time-point was analyzed that could be considered relatively short, these results were in good agreement with the lack of significant differences in the *in vitro* degradation or Ca^{2+} release among BCPC formulations found in the present study. However, a higher dissolution and Ca^{2+} release from the BCPCs *in vitro,* and a higher resorption rate *in vivo*, should not be excluded in longer-term studies, once the more soluble phase was exposed to the surrounding media.

V. Conclusions

Novel biphasic CDHA/β-TCP self-setting cements with a precise control of phase composition were successfully prepared by hydrolysis of a combination of α-TCP and β-TCP. Setting times increased by the addition of β-TCP, which was associated to the fact that the setting of the cement was caused by the transformation of α-TCP to CDHA, whereas β-TCP remained unaltered. The final microstructure consisted of β-TCP particles embedded in the CDHA matrix. This complex microstructure, together with the diminishing SSA with increasing β-TCP content explains the fact that Ca^{2+} release and weight loss were unaffected by the increasing amounts of β-TCP in the timeframe evaluated. However, higher dissolution and Ca^{2+} release from the BCPCs should not be ruled out in longer-term studies, once the more soluble phase is exposed to the surrounding media.

Acknowledgments

Authors acknowledge the financial support in the MAT2012-38438-C03-01 project. The research leading to these results received also funding from the European Commission Seventh Framework Programme (FP7/2007-2013) under the Reborne project (Grant agreement no. 241879). SG acknowledges the Generalitat de Catalunya for funding through a FI Scholarship. CC acknowledges MICINN for the Juan de la Cierva fellowship. Support for the research of MPG was received through the prize ICREA Academia for excellence in research, funded by the Generalitat de Catalunya. The authors acknowledge Trifon Trifonov for his assistance with FIB cross sectioning.

References

[1]P. V. Giannoudis, H. Dinopoulos, and E. Tsiridis, "Bone Substitutes: An Update," *Injury Int. J. Care Injured*, **36S**, S20–7 (2005).
[2]P. Habibovic and K. de Groot, "Osteoinductive Biomaterials – Properties and Relevance in Bone Repair," *J. Tissue Eng. Regener. Med.*, **1**, 25–32 (2007).
[3]R. Z. LeGeros, A. Chohayeb, and A. Shulman, "Apatitic Calcium Phosphates: Possible Dental Restorative Materials," *J. Dent. Res.*, **61**, 343–7 (1982).
[4]W. E. Brown and L. C. Chow, "A New Calcium Phosphate Setting Cement," *J. Dent. Res.*, **62** [67] 2 (1983).
[5]G. Daculsi, R. Z. Legeros, E. Nery, K. Lynch, and B. Kerebe, "Transformation of Biphasic Calcium Phosphate Ceramics *in vivo*: Ultrastructural and Physicochemical Characterization," *J. Biomed. Mat. Res.*, **23**, 883–94 (1989).
[6]L. C. Chow, "Next Generation Calcium Phosphate-Based Biomaterials," *Dent. Mater.*, **28** [1] 1–10 (2009).
[7]R. Z. Legeros, S. Lin, R. Rohanizadeh, D. Mijares, and J. P. Legeros, "Biphasic Calcium Phosphate Bioceramics: Preparation, Properties and Applications," *J. Mater. Sci.: Mater. Med.*, **14** [3] 201–9 (2003).
[8]H. Yuan, Z. Yang, Y. Li, X. Zhan, J. D. de Bruijn, and K. de Groot, "Osteoinduction by Calcium Phosphate Biomaterials," *J. Mater. Sci.: Mater. Med.*, **9** [12] 723–6 (1998).
[9]H. Yuan, H. Fernandes, P. Habibovic, J. de Boer, A. M. C. Barradas, A. de Ruiter, W. R. Walsh, C. A. van Blitterswijk, and J. D. de Bruijn, "Osteoinductive Ceramics as Synthetic Alternative to Autologous Bone Grafting," *Proc. Natl Acad. Sci. USA*, **107** [31] 13614–9 (2010).
[10]D. Le Nihouannen, G. Daculsi, A. Saffarzadeh, O. Gauthier, S. Delplace, P. Pilet, and P. Layrolle, "Ectopic Bone Formation by Microporous Calcium Phosphate Ceramic Particles in Sheep Muscles," *Bone*, **36** [6] 1086–93 (2005).
[11]P. Habibovic, H. Yuan, C. M. van der Valk, G. Meijer, C. A. van Blitterswijk, and K. de Groot, "3D Microenviroment as Essential Element for Osteoinduction," *Biomaterials*, **26** [17] 3565–75 (2005).
[12]A. M. C. Barradas, H. Yuan, C. A. van Blitterswijk, and P. Habibovic, "Osteoinductive Biomaterials: Current Knowledge of Properties, Experimental Models and Biological Mechanisms," *Eur. Cells Mater.*, **21**, 407–29 (2011).
[13]Y. C. Chai, S. J. Roberts, J. Schrooten, and F. P. Luyten, "Probing the Osteoinductive Effect of Calcium Phosphate by Using an *in vitro* Biomimetic Model," *Tissue Eng. Part A*, **1–7** [7–8] 1083–97 (2011).
[14]M. P. Ginebra, E. Fernández, E. A. de Maeyer, R. M. Verbeeck, M. G. Boltong, J. Ginebra, F. C. Driessens, and J. A. Planell, "Setting Reaction and Hardening of an Apatitic Calcium Phosphate Cement," *J. Dent. Res.*, **76** [4] 905–12 (1997).
[15]Joint Committee for Powder Diffraction Studies [JCPDS] –International Center for Diffraction Data, and American Society for Testing and Materials, Powder Diffraction File. Joint Committee for Powder Diffraction Studies, Swarthmore, PA, 1991.
[16]Leibniz Institute for Information Infrastructure, Inorganic Crystal Structure Database (ICSD). Leibniz Institute for Information Infrastructure, Karlsruhe, Germany, 1998
[17]ASTMC266-89, "Standard Test Method for Time of Setting of Hydraulic Cement Paste by Gillmore Needles"; pp. 189–91 in *Annual Book of ASTM Standards, Vol. 04.01. Cement, Lime, Gypsum*. ASTM, Philadelphia, PA, 1993
[18]E. Fernandez, M. G. Boltong, M. P. Ginebra, F. C. M. Driessens, O. Bermúdez, and J. A. Planell, "Development of a Method to Measure the Period of Swelling of Calcium Phosphate Cements," *J. Mater. Sci. Lett.*, **15** [11] 1004–5 (1996).
[19]C. R. Hankermeyer, K. L. Ohashi, D. C. Delaney, J. Ross, and B. R. Constantz, "Dissolution Rates of Carbonated Hydroxyapatite in Hydrochloric Acid," *Biomaterials*, **23** [3] 743–50 (2002).
[20]K. Sariibrahimoglu, S. C. Leeuwenburgh, J. G. Wolke, L. Yubao, and J. A. Jansen, "Effect of Calcium Carbonate on Hardening, Physicochemical

Properties, and *in Vitro* Degradation of Injectable Calcium Phosphate Cements," *J. Biomed. Mater. Res., Part A*, **100** [3] 712–9 (2012).

[21]M. Espanol, R. A. Perez, E. B. Montufar, C. Marichal, A. Sacco, and M. P. Ginebra, "Intrinsic Porosity of Calcium Phosphate Cements and its Significance for Drug Delivery and Tissue Engineering Applications," *Acta Biomater.*, **5**, 2752–62 (2010).

[22]M. P. Ginebra, E. Fernández, F. C. M. Driessens, and J. A. Planell, "Modeling of the Hydrolysis of a-Tricalcium Phosphate," *J. Am. Ceram. Soc.*, **82**, 2808–12 (2004).

[23]D. Hadley, "The Nature of the Paste–Aggregate Interface"; Ph.D. Thesis, Purdue University, 173 (1972).

[24]K. O. Kjellsen, H. M. Jennings, and B. Lagerblad, "Evidence of Hollow Shells in the Microstructure of Cement Paste," *Cement Concr. Res.*, **26** [4] 593–9 (1996).

[25]U. Gbureck, O. Grolms, J. E. Barralet, L. M. Grover, and R. Thull, "Mechanical Activation and Cement Formation of Beta-Tricalcium Phosphate," *Biomaterials*, **24** [23] 4123–31 (2003).

[26]J. Zhang and G. H. Nancollas, "Dissolution kinetics of calcium phosphates involved in mineralization"; pp. 47–62 in *Advances in Industrial Crystallization*, Edited by J. Garside, R. J. Davey and A. G. Jones. Butterworth–Heinemann, London, 1991.

[27]M. A. Lopez-Heredia, M. Bohner, W. Zhou, A. J. Winnubst, J. G. Wolke, and J. A. Jansen, "The Effect of Ball Milling Grinding Pathways on the Bulk and Reactivity Properties of Calcium Phosphate Cements," *J. Biomed. Mater. Res. B: Appl. Biomater*, **98** [1] 68–79 (2011).

[28]E. B. Montufar, Y. Maazouz, and M. P. Ginebra, "Relevance of the Setting Reaction to the Injectability of Tricalcium Phosphate Pastes," *Acta Biomater.*, **9**, 6188–98 (2013).

[29]M. Bohner, R. Luginbühl, C. Reber, N. Doebelin, G. Baroud, and E. Conforto, "A Physical Approach to Modify the Hydraulic Reactivity of Alpha-Tricalcium Phosphate Powder," *Acta Biomater.*, **5**, 3524–35 (2009).

[30]J. M. Illston, J. M. Dinwoodie, and A. A. Smith, *Concrete, Timber, and Metals: The Nature and Behaviour of Structural Materials*. Van Nostrand Reinhold, New York, NY (1979).

[31]M. A. Issa, M. A. Issa, M. S. Islam, and A. Chudnovsky, "Size Effects in Concrete Fracture: Part I, Experimental Setup and Observations," *Int. J. Fracture*, **102**, 1–24 (2000).

[32]S. Yamada, D. Heymann, J. M. Bouler, and G. Daculsi, "Osteoclastic Resorption of Calcium Phosphate Ceramics with Different Hydroxyapatite/β-Tricalcium Phosphate Ratios," *Biomaterials*, **18** [15] 1037–41 (1997).

[33]I. A. Silver, R. J. Murrills, and D. J. Etherington, "Microelectrode Studies on the Acid Microenvironment Beneath Adherent Macrophages and Osteoclasts," *Exp. Cell Res.*, **175** [2] 266–76 (1988).

[34]M. Bohner, J. Lemaıtre, and T. A. Ring, "Kinetics of Dissolution of β-Tricalcium Phosphate," *J. Colloid Interf. Sci.*, **190**, 37–48 (1997).

[35]M. A. Lopez-Heredia, M. Bongio, M. Bohner, V. Cuijpers, L. A. Winnubst, N. van Dijk, J. G. Wolke, J. J. van den Beucken, and J. A. Jansen, "Processing and *in vivo* Evaluation of Multiphasic Calcium Phosphate Cements with Dual Tricalcium Phosphate Phases," *Acta Biomater.*, **8** [9] 3500–8 (2012). □